THE JOURNAL OF PHYSICAL CHEMISTRY Letters

Letter

pubs.acs.org/JPCL

Single Molecule Surface-Enhanced Raman Spectroscopy without Nanogaps

Alyssa B. Zrimsek, Anne-Isabelle Henry, and Richard P. Van Duyne*

Department of Chemistry, Northwestern University, 2145 Sheridan Road, Evanston, Illinois 60208, United States

Supporting Information

ABSTRACT: We provide conclusive proof of single molecule (SM) detection by surface-enhanced Raman spectroscopy (SERS) for discrete Ag triangular nanopyramids prepared via nanosphere lithography (NSL). While the observation of SMSERS has been well-demonstrated using various chemically synthesized nanoparticle substrates, they have a high degree of polydispersity in shape, size, and aggregation state resulting in an interest to develop more reproducible and uniform nanoparticles. Here triangular-based nanopyramids were characterized by scanning electron microscopy to confirm their geometry and interparticle spacing. Then the isotopologue approach with Rhodamine 6G was used to conclusively prove SM sensitivity for the individual nanoparticles. NSL's straightforward, simple fabrication procedure produces large active arrays. Furthermore, the tunable localized surface plasmon resonance makes NSL prepared substrates effective for the detection of resonant molecules by SMSERS.

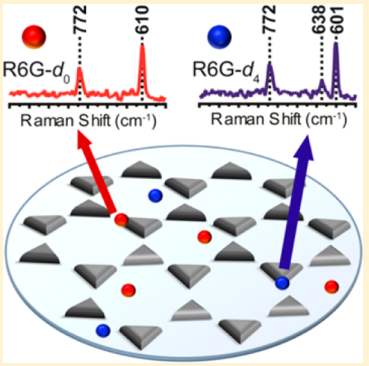

SECTION: Plasmonics, Optical Materials, and Hard Matter

In 1997, considerable interest in surface-enhanced Raman spectroscopy (SERS)[1,2] was renewed with the initial reports of single molecule (SM) detection.[3,4] The interest in SMSERS lies in its analytical capability to detect and identify an analyte down to the SM level with rich fingerprint-like chemical information.[5] The detection of SMs is possible because of the localized surface plasmon resonance (LSPR) or the collective excitation of surface conduction electrons at the nanoparticle surface resulting in enhanced electromagnetic (EM) fields. These enhanced EM fields lead to a large enhancement of the Raman scattering.[6,7] The highest enhancement factors (EFs) are currently believed to occur at the junctions or gaps of nanoparticles known as hot spots, with typical EFs on the order of 10^7-10^8 providing sufficient enhancement for SMSERS.[8−10]

Since the first observation of SM detection, the most commonly utilized nanoparticle substrates have been randomly aggregated colloidal suspensions. Even though the SM capability of colloidal suspensions has been well-demonstrated, they are highly polydisperse in nanoparticle size and geometry.[11−17] Additionally, the salt-induced aggregation of these nanoparticles typically leads to a broad distribution of aggregate sizes, number of members, and interparticle spacing with only a fraction (<1%) of aggregated nanoparticles being SMSERS active.[10]

In order to further advance the field of SMSERS, there is great interest in developing more reproducible and uniform SERS substrates capable of SM detection. For example, nanoengineering and self-assembly have been utilized to control the aggregation of nanoparticles and synthesize aggregates with well-defined nanoparticle gaps.[18−26] Several of these attempts explored the use of nanoparticle dimers, which in principle provide a consistent and controllable EF.[19,20,22−24] Most attempts, however, have been solution based, while other avenues of fabrication remain underutilized. One notable exception is an optical nanoantenna chip shown to be capable of SMSERS by Wang and co-workers.[27] This nanoantenna chip supports the idea that colloidal suspensions are not required for SM detection, and other avenues are worth exploration.

A well-characterized approach for fabricating reproducible SERS-active nanoparticles is nanosphere lithography (NSL).[6,28−33] NSL is a high-throughput technique that creates large arrays of triangular nanoparticles that are inherently similar in shape and size. One major advantage of NSL-derived nanoparticles is the tunability of the LSPR making them versatile for different excitation wavelengths and amenable to the resonance Raman conditions of various analytes of interest.[6,34] These nanoparticles have been shown previously to be capable of supporting EFs of $\sim 10^8$ but are more typically on the order of $\sim 10^7$ in the spectral window used in this experiment.[32] In 2010, a single spectrum of Rhodamine 6G (R6G) was collected from NSL-derived nanoparticles suggesting SM capability.[33] At the time, however, it was not conclusively proven.

The nanofabrication of NSL nanoparticles is straightforward and simple, involving three main steps: (1) self-assembly of polystyrene (PS) spheres into a monolayer on a clean and base treated glass surface, (2) thermal deposition of metal, and (3) removal of PS spheres via tape stripping and sonication in ethanol. By altering the PS sphere size and the thickness of the

Received: August 16, 2013
Accepted: September 12, 2013

   dx.doi.org/10.1021/jz4017574 | J. Phys. Chem. Lett. 2013, 4, 3206−3210

metal deposited the size and aspect ratio of the resulting nanoparticles can be varied, allowing systematic control of the substrate LSPR. For our samples, the LSPR lambda max (λ_{max}) was approximately 546 nm, which was red-shifted from the excitation source of 532 nm to provide optimal enhancement while remaining close to the absorption maximum (λ_{max} = 527 nm) of the R6G isotopologues used to prove SM sensitivity.[32] The LSPR spectrum of a NSL substrate is shown in the Supporting Information (Figure S1). It should be noted that the SM signal observed for all experiments was surface-enhanced resonance Raman scattering (SERRS) but will be referred to as SERS for simplicity.

Figure 1 presents the structural characterization of NSL-derived nanoparticles fabricated on a silicon substrate by scanning electron microscopy (SEM). Based on geometric calculations for a hexagonally close-packed monolayer of spheres, the relationship between PS sphere diameter (D) and interparticle distances (d_{ip}) for NSL-derived nanoparticles is expressed as follows:[29]

$$d_{ip} = \frac{1}{\sqrt{3}}D$$

Based on the equation for a D = 290 nm, the d_{ip} of 167 nm. As determined between 50 nanoprisms in the SEM images, the experimental d_{ip} = 168 ± 7 nm is in close agreement with the expected results. In the top-down view (Figure 1A), the triangular shape of the nanoparticles and their tip-to-tip orientation is clearly observed. While some variation in the sharpness of the tips is seen, there is a large gap between the nanoparticles isolating them from strong electromagnetic coupling.[29] As indicated previously by discrete dipole approximation (DDA) simulations on similarly shaped nanoparticles, the enhanced EM fields are concentrated at the tips of individual triangular nanoparticles with EFs as high as 10^8.[28,35] Figure 1B shows a cross-sectional view of the nanoparticles with a height of 42 ± 7 nm, determined from 34 nanoparticles, consistent with the amount of Ag deposited. To our knowledge, this is the first cross-section of NSL-derived nanoparticles. Based on a previous NSL paper, the speculated geometry of the Ag nanoparticles was a truncated tetrahedron.[31] Figure 1B confirms this geometry provided an accurate description of the fabricated nanoparticles with the observation of nonparallel sides and truncated top. For simplicity we refer to the shape of the nanoparticles as nanopyramids. Figure 1C shows a histogram tabulating 470 tip to tip distances (d_{tt}) of NSL-derived nanopyramids with an average d_{tt} of 83 ± 20 nm. Departure from ideal packing, leading to minor deviation of d_{tt} is believed to result from small variations in the PS sphere size. However, the predominance of relatively large distances observed between nanoparticles indicates that the SM sensitivity is likely the result of individual nanopyramids where the highest enhancement has been shown with DDA calculations to occur at the tips.[28,35] Additionally, it is possible that surface roughness on the individual nanopyramids may contribute to SM sensitivity.

The isotopologue method developed by Dieringer and co-workers was used to prove SM detection with the NSL-derived nanopyramids.[11] Specifically in this experiment, 20 μL of 1 × 10^{-8} M solution containing equal molar amounts R6G-d_0 and R6G-d_4 was applied to the substrates via spin coating. Assuming the entirety of the 20 μL aliquot is evenly dispersed on a 25 mm coverslip, the corresponding surface coverage would be 244 molecules/μm^2. The majority of the substrate surface,

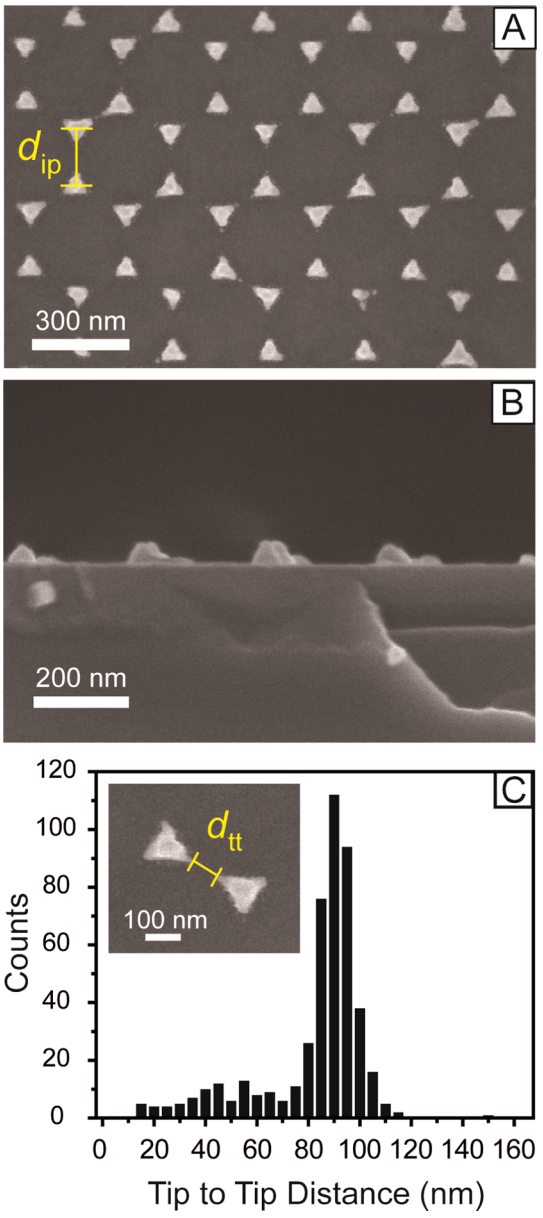

Figure 1. SEM images of NSL-derived Ag triangular nanopyramids fabricated on a silicon substrate with 290 nm PS spheres and 45 nm Ag film in (A) top-down view and (B) cross-sectional view. Interparticle distance (d_{ip}) as indicated in (A) was measured between 50 nanopyramids and was determined to be 168 ± 7 nm. Nanopyramid height as determined from (B) the cross-section of 34 nanoparticles was 42 ± 7 nm. (C) Histogram tabulating 470 tip-to-tip distances (d_{tt}) from SEM images with an average of 83 ± 20 nm.

however, is glass with a nanoparticle surface coverage of only 7.2%.[29] Taking into account this surface coverage and that a typical 1 μm^2 area has ∼32 nanopyramids, as determined from the SEM images, there is <1 molecule per nanoparticle.

The substrates were scanned with a 2 μm step size in the x- and y-directions to limit sample degradation while collecting the SMSERS signal. The peak of interest for distinguishing the identity of R6G-d_0 is 610 cm^{-1}, which differs from the 601 cm^{-1} and 638 cm^{-1} peaks of R6G-d_4.[11] The identification of predominately only one isotopologue in a spectrum versus the identification of both when at equal molar concentrations on the substrate surface was used to prove SM detection based on a binomial Poisson distribution as described previously.[11]

dx.doi.org/10.1021/jz4017574 | J. Phys. Chem. Lett. 2013, 4, 3206−3210

Figure 2 shows representative spectra of R6G-d_0 and R6G-d_4 collected from the NSL substrates indicated by the presence of

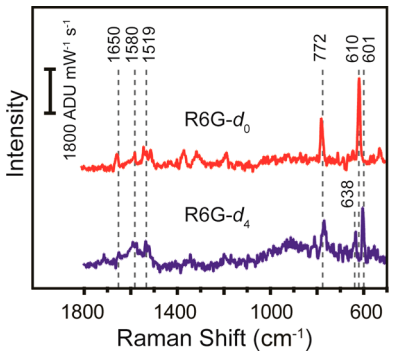

Figure 2. Representative single-molecule spectra of R6G-d_0 and R6G-d_4 collected from NSL-derived triangular nanopyramids. The blue (bottom) spectrum indicates the presence of R6G-d_4 by the observance of the 601 cm^{-1} and 638 cm^{-1} peaks. The red (top) spectrum indicates the presence of R6G-d_0 by the observance of the 610 cm^{-1} peak. In both instances the characteristic peaks from the other isotopologue are not present, indicating single-molecule character. Spectra were collected with λ_{ex} = 532 nm, t_{aq} = 1 s, and P_{ex} = 205 μW and were background corrected for fluorescence due to molecules located on the glass surface between nanopyramids.

the 610 cm^{-1} in the red spectrum and the 601 cm^{-1} and 638 cm^{-1} peaks in the blue spectrum, respectively. In both cases, the peaks of the other isotopologue were not present, indicating SM character. Molecules residing on the glass surface between nanoparticles contributed to fluorescence, which was background subtracted. Spectra retaining the fluorescence background can be seen in the Supporting Information (Figure S2). The identification of SMSERS signal in the presence of fluorescence demonstrates the incredible level of enhancement produced by the NSL-derived nanopyramids.

The spectra can be categorized into three types: only R6G-d_0, only R6G-d_4, or both R6G-d_0 and R6G-d_4. Representative spectra of the three possible events are included in Figure 3A showing only the low frequency region. These spectra were also background corrected for fluorescence. The red spectrum shows only the presence of R6G-d_0 (610 cm^{-1}), the blue spectrum shows only R6G-d_4 (601 cm^{-1} and 638 cm^{-1}), and the green spectrum shows both R6G-d_0 and R6G-d_4 as indicated by the presence of all the characteristic peaks (610 cm^{-1}, 601 cm^{-1}, and 638 cm^{-1}). All three types of events share the 772 cm^{-1} peak, which remains unaltered by deuteration of R6G. The number of instances of each event as identified by the 600 cm^{-1} region is tabulated in Figure 3B. The total number of events was 56, with 47 demonstrating the presence of only R6G-d_0 or R6G-d_4 but not both. The mixed events were 9 of the total 56. The ratio of R6G-d_0-only:both:R6G-d_4-only is 25:9:22, which simplifies to ~2.8:1:2.4. Based on the binomial Poisson distribution for 1 molecule per nanoparticle, the probabilities are 2.5:1:2.5, which is in close agreement with the results.[11] Minor deviation is attributed to a probe volume containing multiple nanopyramids and there being <1 molecule per nanoparticle on the substrate. Additionally, molecules residing on the glass between nanoparticles or on portions of the nanoparticles where there is insufficient enhancement for SM detection is not accounted for in the binomial Poisson distribution and may lead to deviation from ideal statistics. However, the preferential occurrence of events with primarily

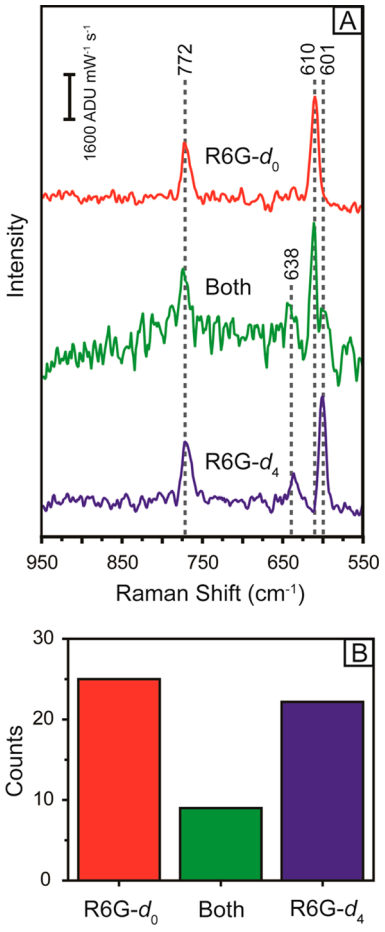

Figure 3. (A) Magnification of the low-frequency region of the three possible events, which are (1) R6G-d_0, (2) RG6-d_4, or (3) both R6G-d_0 and R6G-d_4 collected from NSL-derived triangular nanopyramids with λ_{ex} = 532 nm, t_{aq} = 1 s, and P_{ex} = 205 μW. The spectra were background corrected for fluorescence due to molecules located on the glass surface between nanopyramids. (B) Histogram displaying the occurrence of each event as determined by the 600 cm^{-1} region. Preferential observation of only one isotopologue versus both indicated SM detection.

one isotopologue or the other versus both proves the observation of SMSERS with NSL-derived triangular nanopyramids.

The results presented here indicate that the SMSERS events observed were from individual Ag nanopyramids. Previous electrodynamic calculations on NSL-derived nanostructures indicate that the highest EM fields capable of supporting SM detection occur at the nanoparticle tips.[28,35] Furthermore, unlike traditional aggregated colloidal suspensions with <2 nm nanogaps, the average measured d_{tt} in our system was 83 ± 20 nm. While defects are observed for a few nanopyramids, like the deformed particle in the lower right corner of Figure 1A, the occurrence of these defects is low compared to the number of SM events. Ultimately, the previous simulations and lack of nanometer-scale gaps corroborates that the SMSERS signal originates from SMs located at the nanopyramide tips. Our experiment alone, however, does not rule out the possibility of other sites or provide conclusive proof of the specific locations of the SMs on the nanopyramids.

Figure 4A is a histogram tabulating the peak frequencies for individual SM events of R6G-d_0 (red) and R6G-d_4 (blue). The

dx.doi.org/10.1021/jz4017574 | J. Phys. Chem. Lett. 2013, 4, 3206−3210

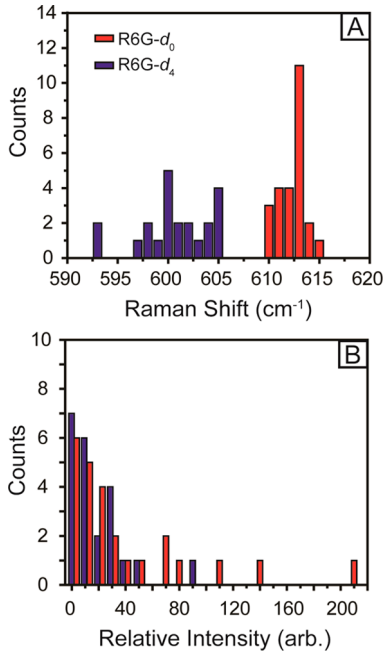

Figure 4. (A) Histogram of the low-frequency peak location for events indicating SM character of R6G-d_0 and R6G-d_4, illustrating the degree of spectral wandering observed for different sites. The isotopologues are clearly distinguishable due to shift ≥5 cm^{-1} between the characteristic peaks of R6G-d_0 and R6G-d_4. (B). Histogram of the characteristic peak intensities from events indicating SM character of R6G-d_0 and R6G-d_4, illustrating the large degree of intensity variation seen between different sites of up to 2 orders of magnitude. R6G-d_0 (red data), and R6G-d_4 (blue data).

difference in peak location is clearly distinguishable between the two isotopologues by a gap of ≥5 cm^{-1}. No frequency shifts were observed for the 772 cm^{-1} peak, indicating that the shifts in the 600 cm^{-1} region resulted from the presence of one isotopologue or the other. The range of peak frequency fluctuation characteristic of SM events observed for R6G-d_0 was 610−615 cm^{-1} and was 593−605 cm^{-1} for R6G-d_4, allowing clear identification of each isotopologue. Additionally, Figure 4B shows the dramatic intensity fluctuations observed for the SM events of R6G-d_0 and R6G-d_4, spanning 2 orders of magnitude. The large intensity fluctuations are consistent with diverse locations of the molecules at a nanoparticle tip, which has a large curvature compared to the molecule size. Tip rounding likely plays a large role in the intensity distribution of Figure 4B as well.

In summary, the data presented here demonstrates that NSL-derived triangular nanopyramids achieve SMSERS without nanogaps using the isotopologue approach with R6G. Due to the large tip-to-tip interparticle distances and through earlier electrodynamic calculations,[28,35] it is likely that the SMSERS events arise at single nanopyramid tips. We also show the first cross-section of triangular nanopyramid arrays prepared via NSL. NSL-derived nanopyramids are advantageous for SMSERS because their tunable LSPR makes them amenable for resonance Raman conditions of various analytes of interest. Furthermore, they are universally available due to their simple fabrication process, large useable array area, and reproducibility.

EXPERIMENTAL METHODS

Preparation of NSL-Derived Triangular Nanopyramids. The NSL-derived nanopyramids were prepared on pretreated glass coverslips (25 mm, #1.5) using piranha etch (3:1 H_2SO_4/30% H_2O_2) followed by base treatment (5:1:1 H_20/NH_4OH/30% H_20_2) with sonication for 1 h to render the surface clean and hydrophilic, respectively.[29] After pretreatment, 4−6 μL of 4 wt % 290 nm PS spheres (Thermo Fisher) were drop-coated onto the glass coverslips. The substrates were allowed to dry in ambient conditions to form large areas of hexagonally close-packed monolayers on the surface of the glass. Using a thermal evaporator (Kurt J. Lesker PVD 75), a 45 nm film of Ag was deposited on the substrates at 1 Å/s and at pressure of ∼10^{-7} Torr. The spheres were removed from the glass surface via tape stripping and ethanol sonication for ∼5 s leaving behind a uniform array of triangular nanopyramids. Before SMSERS measurements were performed, equal molar amounts of R6G-d_0 and R6G-d_4 were dissolved in Mili-Q water (18.2 MΩ·cm) for a final concentration of 1 × 10^{-8} M. Then, 20 μL was spun coat onto the substrate at 1000 rpm for 1 min followed by an additional 2000 rpm for 2 min to ensure complete evaporation of the solution. All samples were used within one day of preparation.

Instrumentation. The SERS measurements were collected on an inverted microscope (Nikon TE300) with an oil immersion objective (Nikon, 100x, NA = 0.5−1.3) with the NA set at 1.0. The signal was collected in a backscattering geometry after which the Rayleigh scattering is filtered with a long-pass filter (Semrock, LP03−532RS-25). The collected signal was analyzed with a 1200 grooves/mm grating and LN_2-cooled CCD (Action 300i, Spec-10 400B). The excitation wavelength was 532 nm (Spectra-Physics, Millenia X) with a power range of 115−205 μW measured at the sample and a spot size of approximately 1 μm^2. All samples were placed in a custom-built flow cell and immersed in a dry N_2 atmosphere. The surfaces of the substrates were scanned using a piezo stage (E-710 Digital PZT) with a step size of 2 μm in the *x*- and *y*-directions. The spectra were collected for 1 s.

SEM Images. SEM imaging was performed on a LEO Gemini 1525 microscope operating at 3 kV. Samples were observed at normal incidence. Cross section imaging was done by mounting the sample on a 90° sample holder.

ASSOCIATED CONTENT

Supporting Information

LSPR spectrum of NSL-derived triangular nanopyramids, and SMSERS spectra showing observed fluorescence. This material is available free of charge via the Internet at http://pubs.acs.org.

AUTHOR INFORMATION

Corresponding Author

*E-mail: vanduyne@northwestern.edu.

Notes

The authors declare no competing financial interest.

ACKNOWLEDGMENTS

We thank Dr. Samuel Kleinman for many helpful discussions on SMSERS. We also gratefully acknowledge the EPIC facility of the Nuance Center for the SEM work performed. This work was supported by the National Science Foundation (CHE-0802913, CHE-0911145, CHE-1152547, and DMR-112162). Dr. Anne-Isabelle Henry acknowledges financial support from DARPA under SSC Pacific grants N66001-11-1 4179, HR0011-13-2-002, and FA9550-08-1-0221. The content of the information does not necessarily reflect the position or the

policy of the Government, and no official endorsement should be inferred.

REFERENCES

(1) Jeanmaire, D. L.; Van Duyne, R. P. Surface Raman Spectroelectrochemistry: Part I. Heterocyclic, Aromatic, and Aliphatic Amines Adsorbed on the Anodized Silver Electrode. *J. Electroanal. Chem. Inter. Electrochem.* **1977**, *84*, 1−20.

(2) Sharma, B.; Frontiera, R. R.; Henry, A.-I.; Ringe, E.; Van Duyne, R. P. SERS: Materials, Applications, and the Future. *Mater. Today* **2012**, *15*, 16−25.

(3) Kneipp, K.; Wang, Y.; Kneipp, H.; Perelman, L. T.; Itzkan, I.; Dasari, R. R.; Feld, M. S. Single Molecule Detection Using Surface-Enhanced Raman Scattering (SERS). *Phys. Rev. Lett.* **1997**, *78*, 1667−1670.

(4) Nie, S.; Emory, S. R. Probing Single Molecules and Single Nanoparticles by Surface-Enhanced Raman Scattering. *Science* **1997**, *275*, 1102−1106.

(5) Le Ru, E. C.; Etchegoin, P. G. Single-Molecule Surface-Enhanced Raman Spectroscopy. *Annu. Rev. Phys. Chem.* **2012**, *63*, 65−87.

(6) Jensen, T. R.; Malinsky, M. D.; Haynes, C. L.; Van Duyne, R. P. Nanosphere Lithography: Tunable Localized Surface Plasmon Resonance Spectra of Silver Nanoparticles. *J. Phys. Chem. B* **2000**, *104*, 10549−10556.

(7) Schatz, G. C.; Van Duyne, R. P. Electromagnetic Mechanism of Surface-Enhanced Spectroscopy. In *Handbook of Vibrational Spectroscopy*; John Wiley & Sons, Ltd: Hoboken, NJ, 2006.

(8) Bosnick, K. A.; Jiang; Brus, L. E. Fluctuations and Local Symmetry in Single-Molecule Rhodamine 6G Raman Scattering on Silver Nanocrystal Aggregates. *J. Phys. Chem. B* **2002**, *106*, 8096−8099.

(9) Le Ru, E. C.; Blackie, E.; Meyer, M.; Etchegoin, P. G. Surface Enhanced Raman Scattering Enhancement Factors: A Comprehensive Study. *J. Phys. Chem. C* **2007**, *111*, 13794−13803.

(10) Camden, J. P.; Dieringer, J. A.; Wang, Y.; Masiello, D. J.; Marks, L. D.; Schatz, G. C.; Van Duyne, R. P. Probing the Structure of Single-Molecule Surface-Enhanced Raman Scattering Hot Spots. *J. Am. Chem. Soc.* **2008**, *130*, 12616−12617.

(11) Dieringer, J. A.; Lettan, R. B.; Scheidt, K. A.; Van Duyne, R. P. A Frequency Domain Existence Proof of Single-Molecule Surface-Enhanced Raman Spectroscopy. *J. Am. Chem. Soc.* **2007**, *129*, 16249−16256.

(12) Dieringer, J. A.; Wustholz, K. L.; Masiello, D. J.; Camden, J. P.; Kleinman, S. L.; Schatz, G. C.; Van Duyne, R. P. Surface-Enhanced Raman Excitation Spectroscopy of a Single Rhodamine 6G Molecule. *J. Am. Chem. Soc.* **2008**, *131*, 849−854.

(13) Etchegoin, P. G.; Le Ru, E. C. Resolving Single Molecules in Surface-Enhanced Raman Scattering within the Inhomogeneous Broadening of Raman Peaks. *Anal. Chem.* **2010**, *82*, 2888−2892.

(14) Etchegoin, P. G.; Le Ru, E. C.; Meyer, M. Evidence of Natural Isotopic Distribution from Single-Molecule SERS. *J. Am. Chem. Soc.* **2009**, *131*, 2713−2716.

(15) Kleinman, S. L.; Ringe, E.; Valley, N.; Wustholz, K. L.; Phillips, E.; Scheidt, K. A.; Schatz, G. C.; Van Duyne, R. P. Single-Molecule Surface-Enhanced Raman Spectroscopy of Crystal Violet Isotopologues: Theory and Experiment. *J. Am. Chem. Soc.* **2011**, *133*, 4115−4122.

(16) Le Ru, E. C.; Meyer, M.; Etchegoin, P. G. Proof of Single-Molecule Sensitivity in Surface Enhanced Raman Scattering (SERS) by Means of a Two-Analyte Technique. *J. Phys. Chem. B* **2006**, *110*, 1944−1948.

(17) Stranahan, S. M.; Willets, K. A. Super-Resolution Optical Imaging of Single-Molecule SERS Hot Spots. *Nano Lett.* **2010**, *10*, 3777−3784.

(18) Ahmed, A.; Gordon, R. Single Molecule Directivity Enhanced Raman Scattering using Nanoantennas. *Nano Lett.* **2012**, *12*, 2625−2630.

(19) Graham, D.; Thompson, D. G.; Smith, W. E.; Faulds, K. Control of enhanced Raman scattering using a DNA-based assembly process of dye-coded nanoparticles. *Nat. Nano* **2008**, *3*, 548−551.

(20) Li, W.; Camargo, P. H. C.; Lu, X.; Xia, Y. Dimers of Silver Nanospheres: Facile Synthesis and Their Use as Hot Spots for Surface-Enhanced Raman Scattering. *Nano Lett.* **2008**, *9*, 485−490.

(21) Lim, D.-K.; Jeon, K.-S.; Hwang, J.-H.; Kim, H.; Kwon, S.; Suh, Y. D.; Nam, J.-M. Highly Uniform and Reproducible Surface-Enhanced Raman Scattering from DNA-tailorable Nanoparticles with 1-nm Interior Gap. *Nat. Nano* **2011**, *6*, 452−460.

(22) Lim, D.-K.; Jeon, K.-S.; Kim, H. M.; Nam, J.-M.; Suh, Y. D. Nanogap-Engineerable Raman-Active Nanodumbbells for Single-Molecule Detection. *Nat. Mater.* **2010**, *9*, 60−67.

(23) Taylor, R. W.; Lee, T.-C.; Scherman, O. A.; Esteban, R.; Aizpurua, J.; Huang, F. M.; Baumberg, J. J.; Mahajan, S. Precise Subnanometer Plasmonic Junctions for SERS within Gold Nanoparticle Assemblies Using Cucurbit[n]uril "Glue". *ACS Nano* **2011**, *5*, 3878−3887.

(24) Vlčková, B.; Moskovits, M.; Pavel, I.; Šišková, K.; Sládková, M.; Šlouf, M. Single-Molecule Surface-Enhanced Raman Spectroscopy from a Molecularly-Bridged Silver Nanoparticle Dimer. *Chem. Phys. Lett.* **2008**, *455*, 131−134.

(25) Voelcker, N. H.; Brodoceanu, D.; Kraus, T.; Cheng, F. Templated Silver Nanocube Arrays for Single-Molecule SERS Detection. *RSC Adv.* **2013**, *3*, 4288−4293.

(26) Wang, H.; Levin, C. S.; Halas, N. J. Nanosphere Arrays with Controlled Sub-10-nm Gaps as Surface-Enhanced Raman Spectroscopy Substrates. *J. Am. Chem. Soc.* **2005**, *127*, 14992−14993.

(27) Wang, D.; Zhu, W.; Best, M. D.; Camden, J. P.; Crozier, K. B. Directional Raman Scattering from Single Molecules in the Feed Gaps of Optical Antennas. *Nano Lett.* **2013**, *13*, 2194−2198.

(28) Haes, A. J.; Haynes, C. L.; McFarland, A. D.; Schatz, G. C.; Van Duyne, R. P.; Zou, S. Plasmonic Materials for Surface-Enhanced Sensing and Spectroscopy. *MRS Bull.* **2005**, *30*, 368−375.

(29) Haynes, C. L.; Van Duyne, R. P. Nanosphere Lithography: A Versatile Nanofabrication Tool for Studies of Size-Dependent Nanoparticle Optics. *J. Phys. Chem. B* **2001**, *105*, 5599−5611.

(30) Hulteen, J. C.; Treichel, D. A.; Smith, M. T.; Duval, M. L.; Jensen, T. R.; Van Duyne, R. P. Nanosphere Lithography: Size-Tunable Silver Nanoparticle and Surface Cluster Arrays. *J. Phys. Chem. B* **1999**, *103*, 3854−3863.

(31) Jensen, T. R.; Schatz, G. C.; Van Duyne, R. P. Nanosphere Lithography: Surface Plasmon Resonance Spectrum of a Periodic Array of Silver Nanoparticles by Ultraviolet−Visible Extinction Spectroscopy and Electrodynamic Modeling. *J. Phys. Chem. B* **1999**, *103*, 2394−2401.

(32) McFarland, A. D.; Young, M. A.; Dieringer, J. A.; Van Duyne, R. P. Wavelength-Scanned Surface-Enhanced Raman Excitation Spectroscopy. *J. Phys. Chem. B* **2005**, *109*, 11279−11285.

(33) Kleinman, S. L.; Bingham, J. M.; Henry, A. I.; Wustholz, K. L.; Van Duyne, R. P. Structural and Optical Characterization of Single Nanoparticles and Single Molecule SERS. *Proc. of SPIE* **2010**, *7757*, 77570J−77570J.

(34) Zhao, J.; Dieringer, J. A.; Zhang, X.; Schatz, G. C.; Van Duyne, R. P. Wavelength-Scanned Surface-Enhanced Resonance Raman Excitation Spectroscopy. *J. Phys. Chem. C* **2008**, *112*, 19302−19310.

(35) Haes, A. J.; Zou, S.; Schatz, G. C.; Van Duyne, R. P. A Nanoscale Optical Biosensor: The Long Range Distance Dependence of the Localized Surface Plasmon Resonance of Noble Metal Nanoparticles. *J. Phys. Chem. B* **2003**, *108*, 109−116.